Stepwise Photodissociation of Vapor-Phase Azomethane

Katherine A. Burton[†] and R. Bruce Weisman*

Contribution from the Department of Chemistry and Rice Quantum Institute, Rice University, Houston, Texas 77251. *Received August 23, 1989*

Abstract: Transient CARS spectroscopy has revealed two kinetic steps in the dissociation of *trans*-azomethane vapor excited with 355-nm light. N_2 and methyl radical photoproducts were detected with nanosecond-scale time resolution through their Raman-active vibrational transitions. Methyl radicals having one quantum of excitation in the ν_2 out-of-plane deformation mode appear within 1 ns after excitation as the first C–N bond of azomethane breaks. The remaining methyldiazenyl radical intermediate then dissociates at the rate of 1.9 (±0.3) × 10^8 s^{-1} to form N_2 and vibrationally unexcited methyl radicals. Similar stepwise photodissociation involving diazenyl intermediates is to be expected for all acyclic azoalkanes.

Azoalkanes (R—N=N—R′) have long been known for their tendency to dissociate into N_2 plus alkyl radicals under the influence of light or heat. In 1929, Ramsperger raised an obvious mechanistic question: during dissociation, do the two C–N bonds break in one step or in two?[1] Despite active research over the past six decades, the mechanisms of azoalkane dissociation remain largely unresolved.[2]

In classifying dissociation pathways we use the terms "stepwise" or "sequential" for a process composed of two stages that are kinetically resolved. Such a mechanism involves a bound intermediate species, which for azoalkanes must be a diazenyl radical (R—N=N·). A "concerted" reaction shows no kinetic evidence of separate steps or an intermediate species, even though examination at higher time resolution might reveal a stepwise process. Finally, "synchronous" dissociation of an azoalkane implies coordinated breaking of the two C–N bonds through a single transition state, with no intermediate species persisting for longer than a vibrational period.

Of the many experimental studies of azoalkane dissociation, most have dealt with thermolysis instead of photolysis, and the photolysis studies have mainly attempted to trace the electronic states involved in photoisomerization and photodissociation,[3] rather than the details of bond breaking. Because any stepwise mechanism requires a bound diazenyl radical intermediate, it is important to consider the stability of this species. Firm spectral evidence for diazenyl radicals is available only from ESR detection of aryldiazenyls.[4] Among studies involving alkyldiazenyls, an early flash photolysis experiment with millisecond resolution failed to detect a methyldiazenyl radical intermediate from azomethane vapor.[5] A more recent flash photolysis investigation of azocumene did report evidence for an alkyldiazenyl radical having a 9-μs lifetime,[6] but serious doubts have been raised about the data interpretation.[7] Turning to theoretical ab initio calculations on simple diazenyl radicals, we find that the dissociations of HNN and CH_3NN are predicted to be exothermic but activated.[8-12] However, because the predicted dissociation barriers are small and sensitive to the computational method, we view the theoretical results on diazenyl radical stability as inconclusive. More recent evidence in favor of diazenyl intermediates in the solution-phase photorearrangement of some cyclic azoalkanes has been reported from product studies.[13,14] Among the many investigations of thermolysis mechanisms, that of Engel and Gerth gave particularly strong evidence for diazenyl radical involvement based on "turnaround" products from the thermal dissociation of an unsymmetrical acyclic azoalkane.[15]

In recent years the method of transient CARS, a kinetic vibrational spectroscopy, has been used to monitor fragments formed in gas-phase azoalkane photodissociation. An early transient CARS study from this laboratory found the formation of photofragments from azomethane to be concerted, in the kinetic sense defined above.[16] The nascent distribution of vibrational energy in the nitrogen product was measured and interpreted as suggesting stepwise dissociation. A subsequent transient CARS study of a highly unsymmetrical azoalkane revealed a measurable delay between the appearance of the first alkyl fragment and that of the second fragment and nitrogen.[17] This result conclusively demonstrated stepwise photodissociation of the unsymmetrical compound under study but left unsettled the question of whether symmetrical azoalkanes might instead undergo synchronous cleavage of their identical C–N bonds.

We report here the results of more refined and thorough transient CARS measurements on azomethane, the prototypical symmetrical azoalkane. These measurements directly reveal sequential breaking of the two C–N bonds and indicate that under the conditions of these experiments, the intermediate methyldiazenyl radical dissociates into CH_3 plus N_2 with a lifetme of 5.3 ± 1 ns.

Experimental Method

Our experiments were performed using the method of transient coherent anti-Stokes Raman spectroscopy (CARS), in which CARS signals from an optically excited sample are measured as a function of Raman frequency and as a function of delay after excitation. CARS is a nonlinear Raman spectroscopy that provides information equivalent to a conventional spontaneous Raman spectrum.[18] Static samples of azomethane vapor at 295 ± 2 K were excited with 355-nm third-harmonic pulses from a Q-switched Nd:YAG laser. This wavelength falls in the weak, diffuse near-ultraviolet absorption assigned to azomethane's lowest lying $^1n\pi^*$ state. When excited in this band, azomethane vapor is known to dissociate into two methyl radicals and N_2 with a quantum yield of 1.[2] Following an electronically controlled nanosecond-scale time delay,

[†] Present address: Naval Research Laboratory, Chemistry Division, Code 6115, Washington, DC 20375.

(1) Ramsperger, H. C. *J. Am. Chem. Soc.* **1929**, *51*, 2134.
(2) Engel, P. S. *Chem. Rev.* **1980**, *80*, 99.
(3) See, for example: (a) Collier, S. S.; Slater, D. H.; Calvert, J. G. *Photochem. Photobiol.* **1968**, *7*, 737. (b) Engel, P. S.; Steel, C. *Acc. Chem. Res.* **1973**, *6*, 275. (c) Chervinsky, S.; Oref, I. *J. Phys. Chem.* **1977**, *81*, 1967. (d) Pritchard, G. O.; Marchant, P. E.; Steel, C. *Int. J. Chem. Kinet.* **1979**, *11*, 951.
(4) Suehiro, T. *Rev. Chem. Intermed.* **1988**, *10*, 101.
(5) Sleppy, W. C.; Calvert, J. G. *J. Am. Chem. Soc.* **1962**, *84*, 4207.
(6) Sumiyoshi, T.; Kamachi, M.; Kuwae, Y.; Schnabel, W. *Bull. Chem. Soc. Jpn.* **1987**, *60*, 77.
(7) Boate, D. R.; Scaiano, J. C. *Tetrahedron Lett.* **1989**, *30*, 4633.
(8) Baird, N. C. *J. Chem. Phys.* **1975**, *62*, 300.
(9) Yamashita, K.; Kaminoyama, M.; Yamabe, T.; Fukui, K. *Chem. Phys. Lett.* **1981**, *83*, 78.
(10) Curtiss, L. A.; Drapcho, D. L.; Pople, J. A. *Chem. Phys. Lett.* **1984**, *103*, 437.
(11) Jensen, H. J. A.; Jorgensen, P.; Helgaker, T. *J. Am. Chem. Soc.* **1987**, *109*, 2895.
(12) Burton, K. A.; Andrews, B. K.; Weisman, R. B. To be published.
(13) Reedich, D. E.; Sheridan, R. S. *J. Am. Chem. Soc.* **1988**, *110*, 3697.
(14) Adam, W.; Dorr, M. *J. Am. Chem. Soc.* **1987**, *109*, 1240.
(15) Engel, P. S.; Gerth, D. B. *J. Am. Chem. Soc.* **1983**, *105*, 6849.
(16) Holt, P. L.; McCurdy, K. E.; Adams, J. S.; Burton, K. A.; Weisman, R. B.; Engel, P. S. *J. Am. Chem. Soc.* **1985**, *107*, 2180.
(17) Adams, J. S.; Burton, K. A.; Andrews, B. K.; Weisman, R. B.; Engel, P. S. *J. Am. Chem. Soc.* **1986**, *108*, 7935.
(18) Tolles, W. M.; Nibler, J. W.; McDonald, J. R.; Harvey, A. B. *Appl. Spectrosc.* **1977**, *31*, 253.

0002-7863/90/1512-1804$02.50/0 © 1990 American Chemical Society

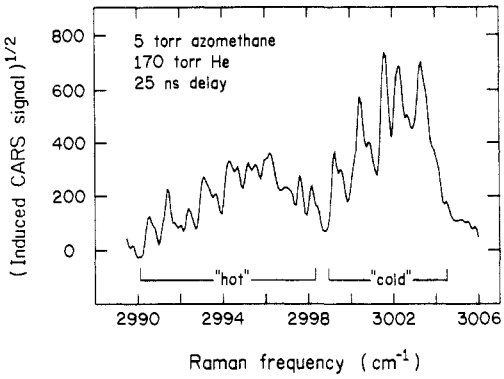

Figure 1. Induced CARS spectrum of methyl radicals measured 25 ns after excitation. The sample contained 5 Torr of azomethane and 170 Torr of helium buffer gas. Band assignments are discussed in the text.

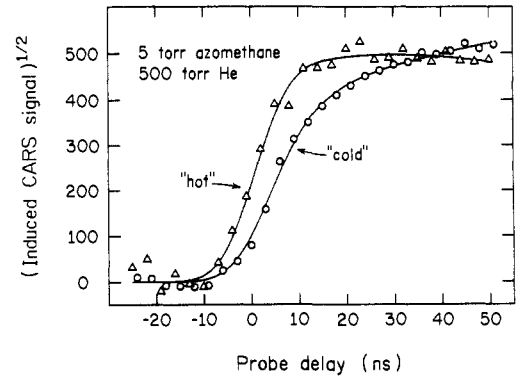

Figure 2. Appearance kinetics of methyl radical photoproducts measured at 2995 cm^{-1} (Δ) and at 3002 cm^{-1} (O). The sample contained 5 Torr of azomethane and 500 Torr of helium buffer gas. The vertical scale units are different for the two sets of data. Solid lines are kinetic fits computed with the models and parameters described in the text.

a second Q-switched Nd:YAG/dye laser system produced the two synchronized pulses used for CARS probing. One of these pulses was the 532-nm second harmonic of the YAG laser. The other was the output of a dye laser pumped with a portion of the 532-nm beam and operated with Rhodamine 640 dye to monitor the N_2 fundamental band or with DCM dye to monitor the C–H stretching region. The frequency difference between the two beams equaled the Raman frequency of the transition that was probed. Because none of the photoproduct species monitored in this work have electronic absorptions near the CARS wavelengths, there was no electronic resonance enhancement of their CARS signal strengths.

The "folded BOXCARS" optical configuration used for these experiments has been described earlier.[19] In brief, the excitation and probe beams were focused into a small volume of the sample region from opposite ends of the 50 cm long sample cell. The probe beams were phase-matched in a mildly noncollinear geometry that prevented nonresonant CARS generation from the cell windows and allowed the weak CARS output beam to emerge at a slight angle to the intense probing beams.[20] This deviation permitted us to use spatial as well as spectral filters to isolate the CARS output light before detecting it with a Hamamatusu R1477 photomultiplier tube. Each resulting charge pulse from the photomultiplier was collected by a gated integrator board, digitized, and then processed by the laboratory computer. The instrumental time response was approximately 8 ns fwhm (limited by the laser pulse widths), and the spectral resolution was ca. 1 cm^{-1} without line narrowing, or 0.2 cm^{-1} with an etalon inserted in the probe YAG oscillator.

CARS data were acquired at the 10-Hz repetition rate of the YAG laser systems. Each excitation pulse typically carried 11 mJ of energy and caused photolysis of approximately 15% of the azomethane molecules in the probed region of the sample cell. During the 100-ms interval between shots, diffusional motion reestablished uniform concentrations of sample and photoproducts throughout the cell. When, after many minutes of irradiation, a significant fraction of the total azomethane sample had been photolyzed or too high a concentration of N_2 had accumulated, the cell was evacuated and refilled with a fresh charge of azomethane. To measure transient vibrational spectra, we set the time delay between photolyzing and probing lasers to a fixed value while scanning the dye laser wavelength (and thereby the probe frequency). Kinetic scans were performed by holding the probe frequency fixed while varying the delay between photolyzing and probing lasers. For both types of scans, background shots with negative delays (probe arriving before excitation) alternated with normal positive delay shots so that the portion of a CARS signal induced by the excitation process could be distinguished from its ground-state component.

Because CARS is a nonlinear spectroscopy, the measured light intensities must be properly processed to give values proportional to the concentration of Raman scatterers. For measurements in the C–H stretching region we subtracted negative-delay signals, representing mainly weak nonresonant backgrounds, from the positive-delay signals. The transient concentrations were taken to be proportional to the square root of this difference. A different data reduction method was required for assessing the induced change in N_2 concentration, because in addition to a nonresonant background there was also a resonant signal from preexisting N_2 formed from prior shots. It is known that the difference in square roots of CARS signals measured at the maximum and the minimum of a band is proportional to the concentration of resonant scatterers,[18,21] in our case N_2. We therefore measured the difference in square rooted CARS signals for positive and negative probe delays as a function of delay time with the probe frequency first set to the band maximum and then to the band minimum. Subtracting these two kinetic scans finally gave the induced change in N_2 concentration as a function of time after excitation.

Results and Discussion

One of our key kinetic findings is based on time-resolved spectroscopy of methyl photofragments in the region of their totally symmetric C–H stretching transition, ν_1. Figure 1 shows part of this transient spectrum measured at 0.2 cm^{-1} resolution in a sample containing 170 Torr of helium buffer gas at a delay of 25 ns after the photolyzing pulse. During this time interval, collisions with helium atoms thermalize the methyl radicals' rotational distributions but leave their vibrational distributions essentially unchanged. As noted on the figure, this spectrum consists of two bands. The higher frequency band is easily identified as the Q-branch of the fundamental $v = 0 \rightarrow 1$ transition in vibrationally unexcited methyl radicals.[22] The observed spectral modulation shows a partially resolved rotational contour. We assign the lower frequency band on the basis of previous experimental reports,[23,24] theory,[25] and band contour analysis[12] to the $v = 0 \rightarrow 1$ transition in methyl radicals that have one quantum of excitation in their ν_2 out-of-plane deformation vibration. At still lower frequencies, we observe further sequence bands corresponding to 2, 3, and 4 quanta of excitation in ν_2.[26]

Of course, it is not surprising that some excitation of the methyl ν_2 mode, whose fundamental frequency is 606.5 cm^{-1},[27] occurs during azomethane photodissociation. Our noteworthy finding is that the two bands of Figure 1 show quite different appearance kinetics. Figure 2 compares the time-dependent concentrations of methyl photofragments containing 0 and 1 quantum of excitation in the ν_2 mode under conditions of rapid rotational thermalization by helium. These data were measured with a probe laser resolution of 1 cm^{-1} at Raman frequencies of 3002 and 2995 cm^{-1}, which are the $v_2 = 0$ and $v_2 = 1$ band maxima for rotationally relaxed samples.

Because our data measure populations in specific ranges of quantum states rather than the total concentration of a chemical species, the kinetic analysis must consider possible contributions from collisional energy relaxation as well as chemical formation. Data for the $v_2 = 1$ methyl hot band were successfully fit by using

(19) Stout, J. E.; Andrews, B. K.; Bevilacqua, T. J.; Weisman, R. B. *Chem. Phys. Lett.* **1988**, *151*, 156.
(20) Shirley, J. A.; Hall, R. J.; Eckbreth, A. C. *Opt. Lett.* **1980**, *5*, 380.
(21) Druet, S. A. J.; Taran, J.-P. E. *Prog. Quantum Electron.* **1981**, *7*, 1.
(22) Holt, P. L.; McCurdy, K. E.; Weisman, R. B.; Adams, J. S.; Engel, P. S. *J. Chem. Phys.* **1984**, *81*, 3349.
(23) Miller, J. T.; Burton, K. A.; Weisman, R. B.; Wu, W.-X.; Engel, P. S. *Chem. Phys. Lett.* **1989**, *158*, 179.
(24) Kelly, P. B.; Westre, S. G. *Chem. Phys. Lett.* **1988**, *151*, 253.
(25) Botschwina, P.; Flesch, J.; Meyer, W. *Chem. Phys.* **1983**, *74*, 321.
(26) Burton, K. A. Ph.D. Thesis, Rice University, 1989.
(27) Yamada, C.; Hirota, E.; Kawaguchi, K. *J. Chem. Phys.* **1981**, *75*, 5256.

a kinetic scheme we will refer to as model 1. The symbols CH_3,

$$CH_3NNCH_3^* \rightarrow CH_3^{**} + X \quad (1)$$

$$CH_3NNCH_3^* \rightarrow CH_3^* + X \quad (2)$$

$$CH_3^{**} + M \rightarrow CH_3^* + M \quad (3)$$

$$CH_3^* + M \rightarrow CH_3 + M \quad (4)$$

CH_3^*, and CH_3^{**} denote respectively methyl radicals with 0, 1, and at least 2 quanta of excitation in the ν_2 mode; $CH_3NNCH_3^*$ is the promptly prepared dissociating state of azomethane; and X symbolizes an unspecified photofragment that is assumed not to lead to CH_3^*. Steps 3 and 4 represent cooling in the ν_2 manifold through collisions with helium or azomethane. In this model only species CH_3^* contributes to the CARS signal at 2995 cm^{-1}. The solid line marked "hot" in Figure 2 shows our fit to the 2995-cm^{-1} data computed by integrating the kinetic equations of model 1 to find $[CH_3^*]$ as a function of time, convoluting with our instrumental response function, and iteratively adjusting the rate coefficients for best agreement with the data. We find that the ratio of k_1 to k_2 is approximately 2.2 and that their sum, $k_1 + k_2$, exceeds 10^9 s^{-1} for samples containing from 500 to 700 Torr of helium plus 0 to 100 Torr of SF_6. Thus, the photochemical production of vibrationally excited CH_3 is found to be prompt on the time scale of these measurements.

The above model could not describe the kinetic data measured at 3002 cm^{-1} for vibrationally cold methyl radicals. Instead, we obtained satisfactory fits using kinetic model 2, below, which contains a non-collisional route for formation of vibrationally cold CH_3.

$$CH_3NNCH_3^* \rightarrow CH_3NN + CH_3^* \quad (1')$$

$$CH_3NN \rightarrow CH_3 + N_2 \quad (2')$$

$$CH_3^* + M \rightarrow CH_3 + M \quad (3')$$

$$CH_3^* + X' \rightarrow \text{products} \quad (4')$$

$$CH_3 + X' \rightarrow \text{products} \quad (5')$$

In model 2, CH_3^* includes all methyls with $v_2 \geq 0$, and step 3′ represents collisional relaxation to form vibrationally cold methyl radicals. The final two steps, which are assumed to have equal rate coefficients, account for chemical reactions that convert the methyl radicals into stable products. We assume that only species CH_3 is detectable at the 3002-cm^{-1} probe frequency.

Applying this kinetic model to data taken at 3002 cm^{-1} gives computed fits such as the solid line marked "cold" in Figure 2. With k_1' set to $>10^9$ s^{-1} (based on the analysis described above for the hot band), k_2' for this scan was found to equal 1.8×10^8 s^{-1}. It is important to determine whether this value actually gives the unimolecular chemical formation rate for a portion of the methyl radicals or instead reflects only a rate-limiting process of collisional energy relaxation. To resolve this point we have used kinetic model 2 to analyze a number of data files measured with various pressures of buffer gases. The triangles in Figure 3 show the resulting averaged k_2' values as a function of helium pressure. It is clear that these values show no trace of the proportional dependence on buffer gas pressure that would reveal rate-limiting collisional relaxation. No points are shown for helium pressures below 400 Torr because those data files could not be adequately fit with kinetic model 2, which includes no step representing rotational relaxation. We infer from this finding that rotational relaxation is rate limiting only for lower buffer pressures and not for the points above 400 Torr. Note that adding 50 Torr of SF_6, a standard polyatomic buffer gas, to 650 Torr of He had virtually no effect on k_2'. Although collisions of hot methyl radicals with SF_6 and He surely produce cold methyls (step 3′), this process corresponds only to the slower rise component of Figure 2, not to the faster rise represented by k_2'. We surmise that the cold methyl radicals show an intrinsic formation rate different from that of the hot methyls and that they therefore must have a different kinetic precursor.

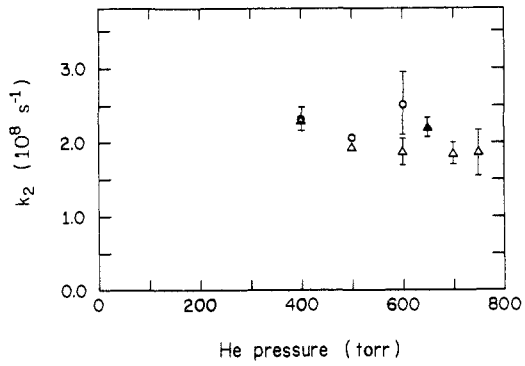

Figure 3. Values of k_2' and k_2'' representing the appearance times of cold methyl radicals (Δ) and N_2 (O) shown as a function of pressure of added helium buffer gas. A total of 51 independent kinetic scans such as those of Figures 2 and 4 are summarized by these points. Values for k_2' and k_2'' were determined from best fits with kinetic models 2 and 3 as given in the text. The filled triangle represents samples containing 50 Torr of SF_6 in addition to 650 Torr of helium. Error bars show the standard deviation of the mean for multiple determinations but do not include systematic errors.

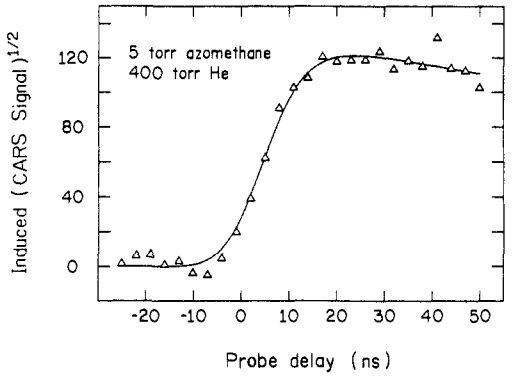

Figure 4. Appearance kinetics of the N_2 photoproduct measured in a sample containing 5 Torr of azomethane and 400 Torr of helium buffer gas. The solid line is a *fit* computed with the kinetic model and parameters discussed in the text.

With a collisional formation route for cold methyl radicals ruled out, what unimolecular alternatives exist? One is radiative relaxation of hot methyl radicals through infrared fluorescence. However, such a process cannot account for our results because vibrational radiative rates are at least five orders of magnitude slower than the measured k_2'.[28] The most likely remaining candidate is shown in model 2 as step 2′: dissociation of the methyldiazenyl radical to give N_2 plus the second methyl photofragment. If this interpretation is correct, then N_2 and cold methyl share a common precursor and must show matching appearance kinetics.

CARS measurement of the nitrogen appearance kinetics is complicated by the fact that, unlike CH_3, N_2 is a stable photoproduct that accumulates in our static sample cell during a run. The primary effect of this changing background is properly compensated for in our data collection process, but there is also a secondary effect that arises from rapid energy deposition in the probed sample volume and a resulting depletion of part of the preexisting N_2 concentration. In kinetic scans, this effect causes an apparent decrease in N_2 concentration on a time scale slower than the formation process. We choose to model this physical concentration decrease through a phenomenological first-order decay coefficient, k_3'' in our kinetic model 3:

$$CH_3NNCH_3 \rightarrow CH_3NN + CH_3 \quad (1'')$$

$$CH_3NN \rightarrow CH_3 + N_2 \quad (2'')$$

$$N_2 \rightarrow \text{"products"} \quad (3'')$$

(28) Lambert, J. D. *Vibrational and Rotational Relaxation in Gases*; Clarendon: Oxford, 1977; p 29.

Here only N_2 is detected by the probing laser.

Figure 4 shows an example of measured N_2 appearance kinetics and a best fit calculated by using model 3 with k_1'' fixed at greater than 10^9 s^{-1}. The k_2'' value used in this fit was 2.1×10^8 s^{-1}. As for the case of vibrationally cold CH_3, we must verify that this appearance rate measures only chemical formation and not rate-limiting energy relaxation. In particular, although only 14% of the N_2 molecules are formed with vibrational excitation,[16] recent evidence indicates a nascent rotational distribution that is very broad.[26] The observed appearance kinetics might therefore be delayed by collisional thermalization into those rotational states that are detected at our probe frequencies. To test this possibility we have measured k_2'' as a function of helium pressure. As was found for the cold methyl data, helium pressures below 400 Torr gave kinetics inconsistent with the model, apparently because rotational relaxation was not rapid compared to step 2. At helium pressures above 600 Torr, CARS nonresonant background levels began to interfere with our measurements. Our averaged results for k_2'' within this limited range of suitable buffer pressures are drawn as circles in Figure 3. They show k_2'' values between 2.1×10^8 and 2.5×10^8 s^{-1} with no significant dependence on helium pressure or azomethane pressure. Within experimental uncertainties, the averaged value of k_2'' agrees with that found for k_2'.

We conclude that the N_2 and cold CH_3 photoproducts share a common precursor whose first-order lifetime is 5.3 ± 1 ns. This common precursor must be the methyldiazenyl radical, CH_3NN, which is formed promptly along with hot methyl in the first step of sequential photodissociation.

Unsuccessful searches for CARS transitions of methyldiazenyl were made at early probe delays in frequency regions expected for C—H and N=N stretching vibrations. Our negative results may be due to an overlap of methyldiazenyl bands with those of azomethane, the unfavorably broad band shapes common for asymmetric rotors, or the modest level of sensitivity provided by CARS probing.

Why do the results reported here differ from those of our earlier transient CARS study of azomethane?[16] One factor is that we have now explored the transient spectra of methyl photofragments using helium buffer gas to quickly relax rotations but not vibrations. This revealed the key difference in appearance kinetics between hot and cold bands. By contrast, the earlier methyl kinetic data were measured only for the cold band in the presence of SF_6 and therefore showed a confusing mixture of direct formation plus vibrational cooling. The second factor concerns setting the proper zero time delay value for kinetic runs monitoring nitrogen appearance. Our most reliable method for setting the time zero uses depletion of a ground-state CARS transition of a directly excited species. Unfortunately, because no suitable ground-state bands were available in the dye region needed for N_2, the earlier work used a time zero transferred from another dye range, thereby incurring a systematic error larger than expected. In the present work we have determined the time zero and instrumental response function more accurately through depletion of a ground-state transition of azomethane-d_6, which has a strong C–D stretching band within the dye range used to monitor N_2. Finally, instrumental refinements have increased the signal-to-noise ratios and permitted more reliable kinetic analysis.

A question that must be considered in any photochemical experiment using pulsed laser excitation is whether the results are distorted by multiphoton absorption processes. In this case, could the two types of methyl radicals actually be separate sets of photoproducts formed from singly and multiply excited azomethane molecules? We note three observations that bear on this question. First, we found no systematic change in the ratio of $v_2 = 0$ to $v_2 = 1$ methyl yields as the excitation intensity was varied by a factor of 4, in contrast to the result expected for a mixture of single and multi-photon products. Second, if the prompt methyl is the product of multiphoton excitation, then it seems very likely that a corresponding amount of nitrogen would also be formed promptly from the multiply excited sample molecules. In fact, we saw no measurable component of prompt nitrogen. The third observation relates to the secondary growth in cold methyl signal (seen in Figure 2) resulting from collisional conversion of vibrationally excited methyls into cold methyls. Through kinetic modeling of the data we have extracted the initial yield ratio of hot to cold methyl radicals and found this ratio to fall within 15% of 1:1, the stoichiometric value demanded by a stepwise mechanism. It is unlikely that an arbitrary mixture of single and multiple photon excitations would so closely match this ratio. We conclude that our results reveal the true one-photon dissociation mechanism.

Conclusions

The ability of transient CARS spectroscopy to detect and distinguish the primary photofragments of azomethane dissociation has provided important insights into this process. Following optical excitation at 355 nm, gas-phase azomethane breaks one C–N bond in less than 1 ns to produce a methyl radical carrying excitation in its ν_2 out-of-plane deformation mode. The resulting methyldiazenyl radical has a first-order lifetime of 5.3 ± 1 ns against breaking its C–N bond to form N_2 and the second methyl radical. This second methyl is predominantly unexcited in its ν_2 mode. The sequential photodissociation may be symbolized

$$CH_3NNCH_3 \xrightarrow{h\nu} CH_3NNCH_3^*$$

$$CH_3NNCH_3^* \xrightarrow{>10^9\ s^{-1}} CH_3NN + CH_3^*$$

$$CH_3NN \xrightarrow{1.9 \times 10^8\ s^{-1}} CH_3 + N_2$$

We found that the methyldiazenyl radical could not be stabilized against dissociation within the available range of collisional conditions, which included approximately 70 hard sphere collisions with He or 3 with SF_6 during the radical's 1/e lifetime.

These kinetic results clearly show that even a completely symmetrical azoalkane undergoes stepwise gas-phase photodissociation similar to that shown earlier for an unsymmetrical azoalkane.[17] Although different diazenyl radicals may have widely varying lifetimes, we expect that photodissociation of all acyclic azoalkanes will be controlled by common features of their excited electronic states, leading to stepwise bond cleavage for this entire class of compounds.

Note, however, that these results probably have no direct bearing on the mechanism of azoalkane thermolysis, since our RRKM calculations suggest that gas-phase photodissociation does not proceed from the vibrationally excited ground electronic surface.[12] In addition, the findings reported here may not apply to the small residual yields of photodissociation known to persist at very high buffer pressures and in solution, because that channel may involve electronic states that are not dominant in the gas-phase process.[3]

Several important mechanistic problems remain. One is uncovering the electronic states and structures that lead to azoalkane photodissociation and photoisomerization in various environments. Another is understanding the differences between the photochemistry of acyclic and cyclic azoalkanes. A third is interpreting the detailed dissociation dynamics, including factors governing diazenyl lifetimes and the disposal of energy in photofragments. We plan to present further experimental and theoretical results on these topics in the near future.

Acknowledgment. Research funding has been provided by the National Science Foundation and the Robert A. Welch Foundation. Acknowledgement is also made to the donors of the Petroleum Research Fund, administered by the American Chemical Society, for partial support of this work. We are very grateful to P. S. Engel, J. S. Adams, and B. K. Andrews for stimulating discussions and comments and for essential azomethane samples.

Registry No. *trans*-$CH_3N{=}NCH_3$, 4143-41-3; $CH_3N{=}N^*$, 64287-49-6; CH_3^*, 20741-88-2.